STUDY ON THE PREPARATION OF COLUMN-CELL AND ITS INFLUENCE ON MECHANICAL PROPERTIES BY DEEP DRAWING

LI Fengkai [1], DENG Anzhong[2], RONG Xiang[1], CHEN Ke[1], LI Haonan[1]

ABSTRACT: A thin-walled semi-ellipsoidal shell unit was designed. The column-cell was prepared by deep drawing process and the forming process was numerically simulated. The influence of deep drawing on the wall thickness and pre-strain of the column-cell cell was discussed, the effect of pre-strain on mechanical properties of 0Cr18Ni9 stainless steel and T2 copper was also intensively studied. The results show that the deep drawing process will cause wall thickness of the column-cell to be thinner, and the longer the deep drawing distance is, the thinner the thickness is; The longer the thickness is, the greater the flow stress under the same strain, and the smaller the elongation after breaking for the same metal sheet material; The pre-strain distribution of the sheet material after deep drawing is significantly uneven, and larger plastic strain is produced at deeper parts. Under the same deep drawing condition, the maximum pre-strain of T2 copper column-cell was significantly higher than that of 0Cr18Ni9 stainless steel. And the pre-strain has significant effect on the plastic deformation ability of the metal material. When the pre-strain increases, the yield strength of the material increases and the elongation at break decreases.

KEY WORDS: deep drawing forming process; column-cell; numerical simulation; pre-strain

1 INTRODUCTION

The column cell, similar to a thin-walled metal tube, is a cost effective buffering energy-absorbing configuration with advantages of long and big range deformation under explosive blast (Sun et al., 2017; Rezvani and Jafarian, 2017; Altin et al., 2017), which is able to reduce the peak load of axial impact effectively. As an energy absorbing effective thin-walled configuration, it enjoys promising application prospect in the fields of aerocraft and protection works. However, due to its special curved surface, mutability, low stiffness and thin thickness, its machining dimension accuracy and stability are difficult to control (Tang, 2012; Panchagnula and Simhambhatla, 2018; Xiong et al., 2017; Masmali and Mathew, 2017), in addition, different processing technics exert great influences on the performance of the thin-walled components. In recent years, the researches on the processing technics and performance of the thin-walled components have been deepening both domestically and abroad. Cao (2014) combined the methods of digital modeling, finite element simulation and experimental verification to study the deformation prediction technology of five axis machining for thin-walled complex surface of titanium alloy. Finally he established the flexible iterative deformation prediction algorithm for the machining thin-walled complex surface based on the cutting balance and the prediction was in line with the facts. Combining the methods of simulation and experiment and taking thin-walled frame parts as the subject, Jiang (2014) conducted the research on the control method of machining accuracy of complex thin-walled parts, which provided the basis for controlling machining accuracy of complex thin-walled parts and residual stress. Zhang et al., (2012) worked out the thin-walled aluminum alloy shell by combining the processes of hot spinning formation, machined hemispherical surface and final spinning formation. His research showed that the formed spinning parts with fine crystalline grains had enhanced the yield strength by 20MPa while the plasticity remained fine. Yin et al., (2013) studied the parameters of preformed parts, such as shapes, passes and spinning tracks. He found that the precision of thin-walled parts formation was significantly influenced by the accuracy for size and shape of the stamping preformed parts, the general spinning passes and the reduction rate of thickness of power spinning during the spinning process. Aimed at Aluminum Alloy Zede deformation of thin-walled shell parts, established the mathematical model of spherical shell deformation and finite element

[1]Department of chemistry and material engineering, Logistics Engineering University, Chongqing 401331, China

[2]Department of engineering management, Chongqing 401331, China)

Email: lfkdly@qq.com

simulation model by He and Tian (2017). Reduce effectively the deformation of spherical shell by controlling the vacuum and change the clamping contact position, improve the dimensional accuracy of the processing.

Firstly, a thin-walled semi-ellipsoidal shell unit was designed based on the current research in this thesis. The stamping process—the deep drawing process was selected for making column-cells with different materials and thicknesses. At the same time, the forming process of finite element simulation was used for a deeper study on the influences which the pre-strain caused by the forming process exerted on the material characteristics. The reasons for the rule generation were explained as well. The research findings were of great theoretical significance and practical application value in accurate forming technology of thin-walled shells.

2 DESIGNING AND PREPARING FOR THE COLUMN-CELLS

2.1 Designing of column-cells

2.1.1 Designing of Geometric Configuration

The column cell configuration designed and studied in this thesis was ellipsoid shell configuration as shown in figure 1. Its longitudinal section is semi-ellipse, the transversal section was round, r_1 is the equatorial radius, r_2 is the polar radius and t is the average wall thickness. The size of the column is: The equatorial radius r_1=17mm, the polar radius r_2=21mm, t=0.3, 0.5, 0.7 and 0.9mm.

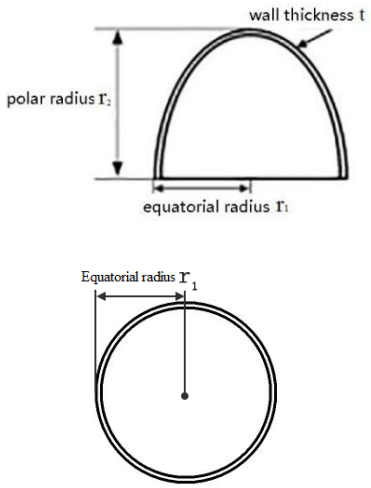

Figure 1. Geometry Description of the Column Cell

2.1.2 The Base Materials

Two base materials for column cells were selected: 0Cr18Ni9 stainless steel and T2 copper. Steel 0Cr18Ni9 has the structure of austenite and the austenite has face centered cubic structure. The structure has many lattice slip systems so it has good plasticity and low yield strength. T2 Copper is commercially pure copper. It is red for the oxide film formed on its surface and it has face centered cubic structure both under high temperature and normal temperature. Both 0Cr18Ni9 stainless steel and T2 copper have good plastic formability and corrosion resistance and they are widely used in industrial production.

2.2 Preparing column-cells

2.2.1 Preparing column-cells by deep drawing process

The trial column cell parts selected for this research can be formed by thin sheet deep drawing. Because the friction force between the mould and the sheets is high during the forming and the sheets are often broken for the plastic deformation, one-step formation is not adoptable. Therefore, the process is divided into three steps: pre-drawing formation, formation adjustment and edge cutting. Pre-drawing formation refers to the deep pre-drawing formation for the sheets with the hydraulic press. During the pre-drawing formation, the hydraulic press shall run with constant speed and the temperature of the trial parts shall be constant, in order to avoid destroying the molecular arrangement of the base materials for column cells and changing the mechanical property of the base materials for column cells. Figure 2(a) is a chart for pre-drawing formation. As shown in the figure as follows, a circular opening of Ø5mm is made for the bottom mould. This is to avoid that the bottom mound may be broken for high friction at the position of the opening during the forming. As shown in figure 2(b), the formation adjustment aims to the circular opening appearing at the end after the pre-drawing formation. After the formation adjustment, the trial part is in line with the ellipsoid shell configuration. Edge cutting is to separate the deep drawing formed part from the sheet and get the standard trial column-cell parts as shown in figure 2(c) .

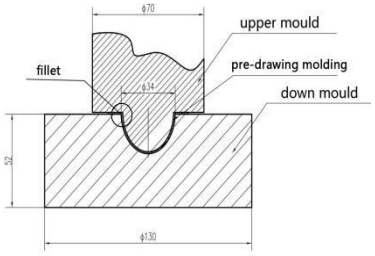

(a) Pre-Stretch forming

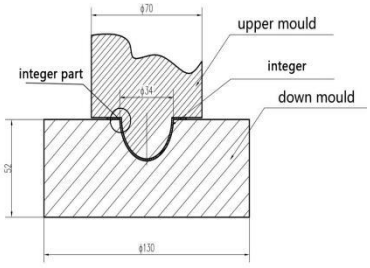

(b) Integer

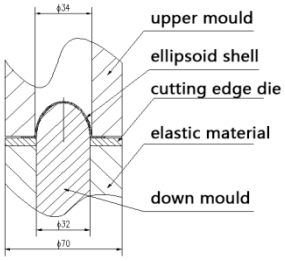

(c) Cutting edge

Figure 2. Machining Process of the Specimen

2.2.2 Research of Digital Simulation

During the actual preparing process, the processing technics are mainly controlled by qualitative analysis and some technological measures based on previous experience. As a result, the efficiency and precision are not high. In order to ensure the processing quality of the column cells, digital simulation is introduced in this section. This method is to simulate the deep drawing formation of the column cells and pre-identify the defects during the column cell formation, such as cracking, crinkling and nonuniform wall thickness. In this way, the processing efficiency and precision are improved.

(1) Establishing finite element model

The main performance parameters of column cells after processing, such as wall thickness and pre-strain of the materials at different parts etc., are determined by the first step of the forming process—pre-drawing formation. Therefore, a model for finite elements is established during the simulated pre-drawing process. Because the sheet is deformed as axial symmetry during the pre-drawing forming, in order to save the calculation time, the model for finite elements is simulated by 1/2 of the actual mould size, as shown in figure 3. The model for finite elements mainly include an upper mould, a bottom mould, a blank holder and the sheet. The sheet is simulated according to the complete integral Belytschko-Tsay shell element algorithm. 5 integration points were adopted along the direction of thickness and the unit characteristic length is taken as 0.06 mm. The type of upper mould unit is set as rigid body and the degrees of freedom to all the directions except the axial side are restricted. The speed of the upper mould axis is 4 m/s; the type of bottom mould unit is set as rigid body as well and the degrees of freedom to all the directions are restricted. During the analysis, the algorithm of CONTACT-AUTOMATIC-SINGLE-SURFACE is adopted to study the contact between the sheet and the upper mould and the contact between the sheet and the bottom mould. Both the coefficient of kinetic friction and the coefficient of static friction are taken as 0.1.

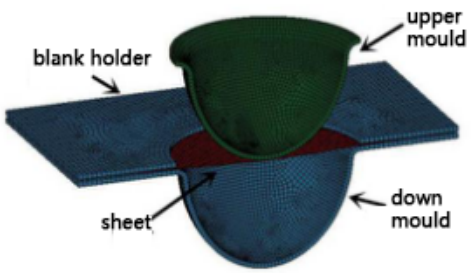

Figure 3. The 1/2 Finite Element Model

(2) Setting the Material Parameters

The mould is analyzed according to the MAT-RIGID model in LS-DYNA in this paper. This model requires for related parameters of actual mould, including density, Poisson ratio and Young modulus, as shown in table 1. The parameters of basic processing performance for 0Cr18Ni9 stainless steel and T2 copper are shown in the table. The material model of No. 123 is analyzed according to MAT-MODIFIED-PIECEWISE-LINEAR-PLASTICITY in LS-DYNA. This material model can be used to define arbitrary stress – strain curve. Thus, the actual stress – strain curve of the 0Cr18Ni9 stainless steel and T2 copper obtained from the experiment can be used in the material model.

Table 1. Processing Performance Constant

Material	Density (kg/m^3)	Modulus of Elasticity/GPa	Poisson ratio
0Cr18Ni9	7.93×103	193	0.29
T2	8.90×103	125	0.35

In the stamping process, due to the certain moving speed of the upper mould, the influence on material performance exerted by the strain rate shall be taken into consideration. As for the 0Cr18Ni9 stainless steel, while the effect of strain rate is considered, the model of Cowper-Symonds which is currently widely used can be selected (Wang X.S et al, 2013).

$$\sigma_Y(\varepsilon_P^{eff},\dot{\varepsilon}) = [1+\left(\frac{\dot{\varepsilon}}{C}\right)^{\frac{1}{P}}] \cdot \sigma_Y^S(\varepsilon_P^{eff}) \quad (1)$$

In the model, ε_P^{eff} stands for equivalent plastic strain, $\sigma_Y(\varepsilon_P^{eff},\dot{\varepsilon})$ stands for the stress value corresponding to the strain rate of $\dot{\varepsilon}$ and the stress ε_P^{eff}, $\dot{\varepsilon}$ refers to equivalent plastic strain rate, C and P refer to strain rate parameter, $\sigma_Y^S(\varepsilon_P^{eff})$ stands for the quasi-static stress value for corresponding strain ε_P^{eff}.

According to the related bibliography (Zhu X.Q and Liu H., 2009), the strain rate parameters of the 0Cr18Ni9 stainless steel are:

$$\begin{cases} C = 100s^{-1} \\ P = 10 \end{cases} \quad (2)$$

As for T2 copper, it is clarified in related research (Liu et al., 2015): When the strain rate was lower than 14000s^{-1}, there weren't obvious changes for the yield stress of the material. Therefore, this material can be taken as strain rate insensitive material.

3 INFLUENCES ON MATERIAL PERFORMANCE EXERTED BY DEEP DRAWING FORMING

3.1 Thickness Changes

The deep drawing forming process may result in serious thickness reduction in a certain part of the wall of the column cell. The trial column cell formed by deep drawing is cut along the longitudinal section as shown in figure 4 and the wall thickness is measured. The measure points are determined every 2.5 mm from the top along the direction of polar radius and there are 8 measure points taken. The detailed chart is shown as figure 5. The thickness of the front sheet formed by deep drawing is defined as the standard thickness t0, the wall thickness at different parts of the deep forming column cell is the actual thickness t, and the reduction rate r is: $r = (t_0 - t)/t_0$

Figure 4. The Longitudinal Section of Column Cells

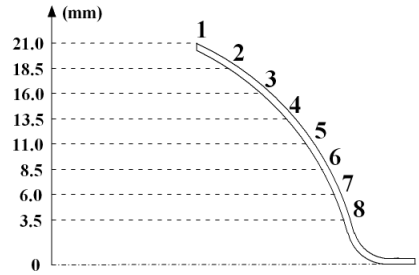

Figure 5. Schematic Diagram of Thickness Measurement point

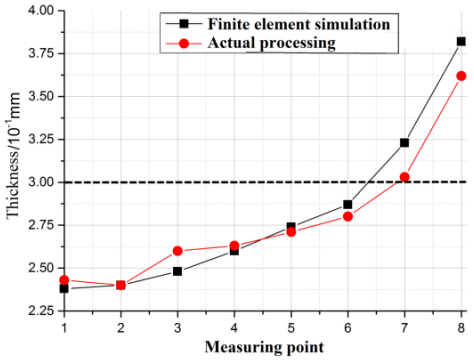

(a) 0.3mm 0Cr18Ni9 stainless Steel

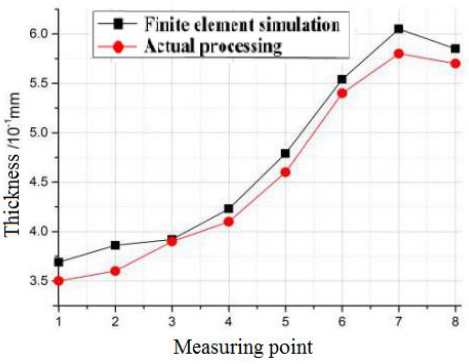

(b) 0.7mm 0Cr18Ni9 stainless Steel

Figure 6. The thickness of Stainless Steel Specimens in Different Measurement Points

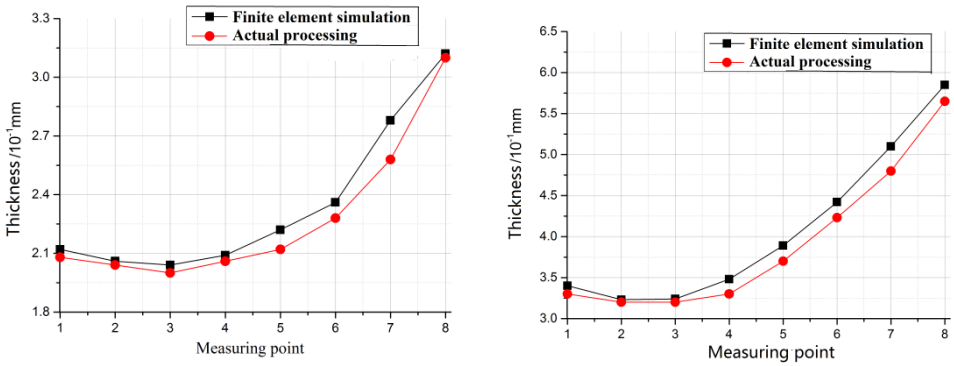

(a) 0.3mm T2 copper **(b) 0.7mm T2 copper**

Figure 7. The Thickness of Copper Specimens in Different Measurement Points

From figure 6 and 7, it can be seen that the results from the finite element simulation are in line with the actual processing results because the maximum deviation is not more than 8%. Thus, the effectiveness of the finite element models is verified. In addition, it can be seen from Fig. 6, the thickness at the end both deep drawing trial column cells for o.3mm stainless steel and copper are thicker. This is because the circumferential compressive stress at the deep drawing part is higher than the radial tensile stress during the drawing process and the gaps between the upper mould and the bottom mould are bigger than the sheet thicknesses so "crinkling" appears. "Wrinkling" appears at the midpoint positions of each sheet side and the stress is concentrated. The figure 8 is the von-mises stress picture and actual picture of the steel sheet formed by deep drawing.

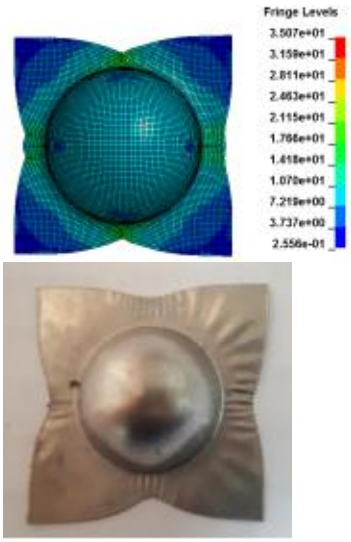

Figure 8. The 0.3mm Stainless Steel After Deep Drawing Forming

As for the metal sheets with thicknesses of 0.5mm and 0.7mm, there is no "wrinkling" happened during the deep drawing forming process. The longer the drawing distance is, the thinner corresponding wall is. figure 9 shows the wall thickness reduction rate for 0.5mm stainless steel sheet and copper sheet formed by deep drawing. It is found that the copper cell has more serious problems of wall thickness reduction than the stainless steel and the wall thickness at different positions are not constant.

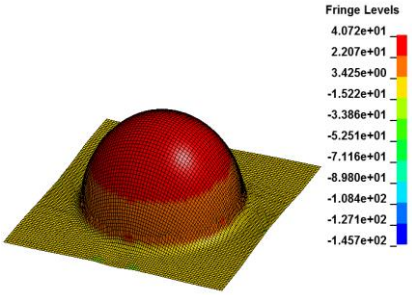

(a) 0.5mm stainless steel

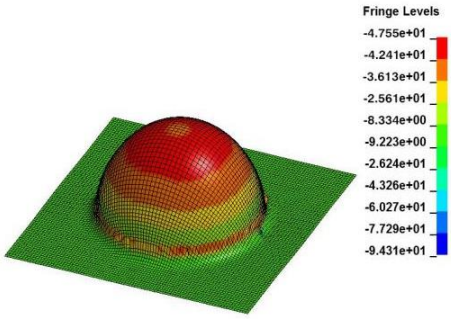

(b) 0.5mm copper

Figure 9. The Thickness Reduction of 0.5mm Stainless Steel and Copper after deep Drawing Forming

3.2 Pre-strain Changes

The deep drawing deforming causes the plastic deformation of two metal materials, 0Cr18Ni9 stainless steel and T2 copper, and this brings the pre-strain of the base materials of the column cells. Such pre-strain changes the structure of the base

materials and results in the changes in their mechanical property. Figure 10 is the Nephogram of Equivalent Plastic Strain Distribution after the deep drawing forming for the sheet metal of 0.5mm 0Cr18Ni9 stainless steel and T2 copper. It can be seen from Fig. 10 that the pre-strain distribution of the sheet metal after deep drawing forming shows obvious inhomogeneity. At the place where the drawing is deeper (such as the top of the column cell), the plastic pre-strain is bigger. From the top to the bottom of the column cell, the plastic pre-strain is reducing gradually; The maximum equivalent plastic strain for the whole 0Cr18Ni9 stainless steel column cell is about 0.52 while the minimum is about 0.20; The maximum equivalent plastic strain for the whole T2 copper column cell is about 0.55 while the minimum is about 0.21.Through the comparison, it is found that the maximum equivalent plastic strain of T2 copper column cell is significantly higher the one of 0Cr18Ni9 stainless steel column cell under the same conditions of deep drawing forming. The reason is: When the upper mould moves down and touches the sheet metal, the external sheet metal flows into the cavity of the concave die constantly. Because the yield stress of copper is obviously less than the yield stress of stainless steel, the fluid ability of the external copper sheet to overcome the friction between the copper sheet and the mould is less than the one of the stainless steel and this results in the bigger tensile degree of the part where the copper sheet touches the upper mould. Thus, the maximum equivalent plastic strain is bigger. This also explains why the wall thickness reduction rate of the T2 copper column cell is higher.

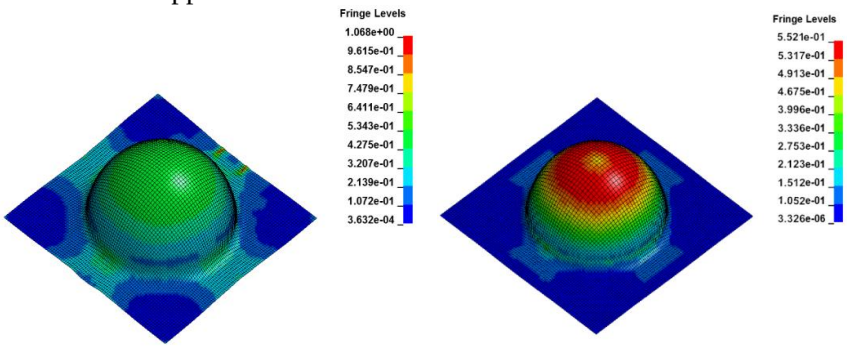

(a) 0.5mm Stainless Steel **(b) 0.5mm Copper**

Figure 10. Nephogram of Equivalent Plastic Strain Distribution of 0.5mm 0Cr18Ni9 Stainless Steel and T2 Copper

3.3 The Influences on the Mechanical Property of 0Cr18Ni9 Stainless Steel and T2 Copper Exerted by Pre-strain

The research shows that the deep drawing forming process caused changes in the pre-strain of the base materials at different places of the column cells. Under the normal temperature, the material pre-strain produces the lattice deformation, which causes the changes of plastic formation indicators of yield strength and elongation at break and these indicators changes along with the pre-strain changes. Therefore, in order to better analyze the influences on the mechanical property of the column cells exerted by the deep drawing forming process, deeper research on the effects of pre-strain on the material mechanical property shall be done.

3.3.1 The Static Tensile Test on Sheet Metal Material under Pre-Strain

The static tensile test on sheet metal material under pre-strain includes two stages: The first stage is exerting pre-strain and the second stage is reloading after uniaxial tensile test. Exerting pre-strain means exerting tensile pre-strain on a group of standard metal tensile pieces and unloading until the tension reaches certain pre-strain. Reloading after uniaxial tensile test means drawing the metal pieces again along the original drawing direction after unloading until the metal pieces are broken. The picture of the test process is as follows:

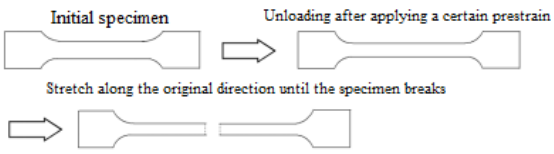

Figure 11. The Process of Test

3.3.2 Observation on Metallographic Phase

MR200 metallurgical microscope is used to observe the metallographic phase of the metal

tensile test samples. The surface for observation is the longitudinal section at the center of the original gauge length. To study the micro-changes of the sheet metal with different thickness under different situations of pre-strain, metallographic phases of different thickness and under different situations of pre-strain are observed.

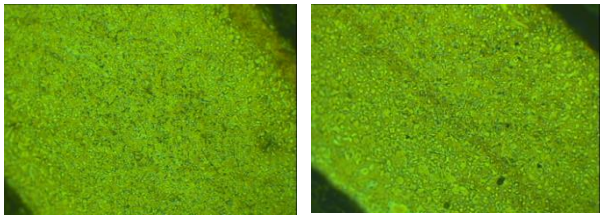

(a) 0.3mm **(b) 0.5mm**

Figure 12. Metallograph of 0Cr18Ni9 Stainless Steel with Different Thickness

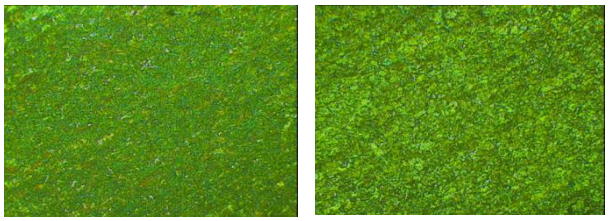

(a) 0.3mm **(b) 0.5mm**

Figure 13. Metallograph of T2 Copper with Different Thickness

Figure 12 and 13 are the pictures of metallographic phase. They are taken from the longitudinal sections of standard metal tensile test sample for 0Cr18Ni9 stainless steel and T2 copper. As seen from the metallograph, as the thickness of samples is reducing, the grain size of the material is getting smaller. As known, the grain size has significant influences on the mechanical property. This influence is essentially produced by the grain boundary area. The smaller the grain size is, the bigger the grain boundary area is, and the more effects on the mechanical property are exerted. As for the mechanical property of the metal under normal temperature, generally speaking, the smaller the grain is, the higher the strength and hardness are. Here is the reason: as the grain size is getting smaller, the plastic deformation can be distributed into more grains, which makes the plastic deformation more constant and the internal stress concentration weaker. As a result, the thickness of 0Cr18Ni9 stainless steel and T2 copper is reducing and the yield strength is increasing.

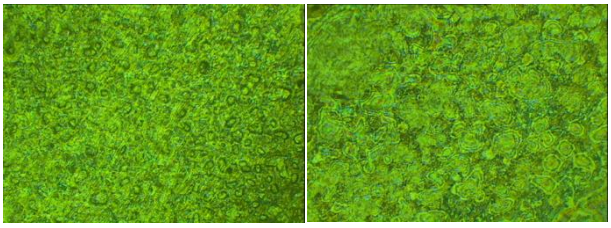

(a) Pre-strain 0.1 **(b) Pre-strain 0.2**

Figure 14. Metallograph of 0Cr18Ni9 Stainless Steel with Different Pre-strain

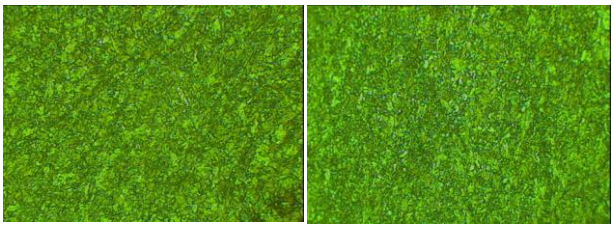

(a) Pre-strain 0.1 **(b) Pre-strain 0.2**

Figure 15. Metallograph of T2 Copper with Different Pre-strain

Figure 14 and 15 are the pictures of metallographic phase. They are taken from the longitudinal sections of standard metal tensile samples for 0Cr18Ni9 stainless steel and T2 copper. The higher the pre-strain is, the bigger the grain size is.

3.3.3 Curve Analysis on Stress-Strain

Figure 16 is the stress-strain curve drawn according to the actual stress-strain obtained through reloading after the pre-strain is exerted on standard metal tensile samples for T2 copper with different thicknesses. It is seen that the true stress-strain curve is influenced a lot by the initial pre-strain under the uniaxial tensile test. Compared with the one without pre-strain, the actual stress is increasing considerably. There are two factors which cause stress increasing:

On the one hand, by comparing the pictures of metallographic phase, it is known that the higher the pre-strain is, the bigger the grain size is. In addition, the thickness of the samples is reducing after exerting the pre-stress. Both effects cause the number reduction of the grains on the thickness direction. However, the grains on the thickness direction have great effects on the actual stress of the samples in the uniaxial tensile test: When there are more grains on the thickness direction, the grain distribution is constant; when the grain distribution is reduced to a certain extent on the thickness direction of the samples, plastic deformation only easily happen to the grains which are on the favorable direction in the uniaxial tensile test. Therefore, the higher the pre-strain is, the higher the

yield stress is, under the same strain.

On the other hand, the higher the pre-strain is, the higher the actual stress is in the tensile test for the samples with same thickness. The main reason for this is the micro-structure change in materials caused by the pre-strain: Exerting pre-strain on the samples increases the dislocation density of the materials and enhance the interaction caused by the dislocation. Then various stable and nonstable dislocation patterns are formed and work hardening happens. However, along with the increasing pre-strain, the dislocation density inside the material structure increases dramatically and this greatly enhances the plastic deformation resistance.

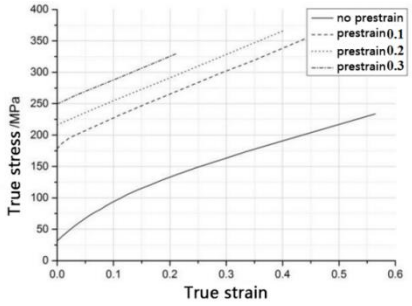

(a) 0.7mm thickness sample

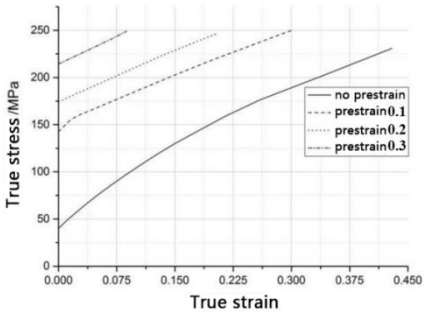

(b) 0.5mm thickness sample

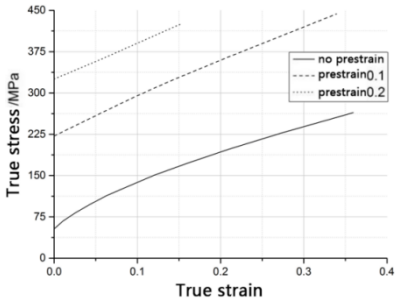

(c) 0.3mm thickness sample

Figure 16. The True Stress-strain Curve of T2 Copper Samples with Different Thickness and Pre-strain

3.3.4 Analysis on Yield Strength

The yield strength is mainly used to indicate the stress with which the metal materials resist the initial plastic deformation and it is one of the most important indicators for metal materials. Table 2 shows the yield strength in uniaxial tensile test for samples of T2 copper and 0Cr18Ni9 stainless steel under the pre-strain. It is concluded by the result that the yield strength is getting higher along with the increasing pre-strain.

Table 2. The Yield Strength of T2 Copper and 0Cr18Ni9 Stainless Steel Under the Pre-strain

Material	Thickness /mm	Pre-strain	Yield Strength/MPa	Material	Thickness/mm	Pre-strain	Yield Strength/MPa
T2 Copper	0.3	0	53.24	0Cr18Ni9	0.3	0	521.86
		0.1	221.87			0.1	611.52
		0.2	325.32			0.2	682.08
	0.5	0	40.01		0.5	0	447.54
		0.1	123.25			0.1	530.03
		0.2	173.98			0.2	623.52
		0.3	214.24			0.3	745.23
	0.7	0	28.91		0.7	0	379.78
		0.1	169.22			0.1	543.5
		0.2	210.35			0.2	639.8
		0.3	245.63			0.3	736.3
	0.9	0	31.25		0.9	0	347.73

Material	Thickness /mm	Pre-strain	Yield Strength/MPa	Material	Thickness/mm	Pre-strain	Yield Strength/MPa
		0.1	178.11			0.1	522.17
		0.2	216.35			0.2	618.81
		0.3	249.50			0.3	723.29

3.3.5 Elongation Analysis

The plastic deformation capacity of the standard metal drawing sample before breaking is called plasticity. The plasticity can be indicated by the elongation at break. However, in the actual works, apart from the elongation at break δ, there is a kind of uniform elongation δ', which indicates the percentage between the total elongation $\Delta L'$ and original gauge length L at the stage of uniform elongation. Because the metal drawing sample used in this research is comparatively thin, there is no obvious constriction part on the stress-strain curve before breaking, it can be concluded that the elongation at break is approximately equal to the uniform elongation, it is shown as: $\delta = \frac{\Delta L}{L} \times 100\%$.

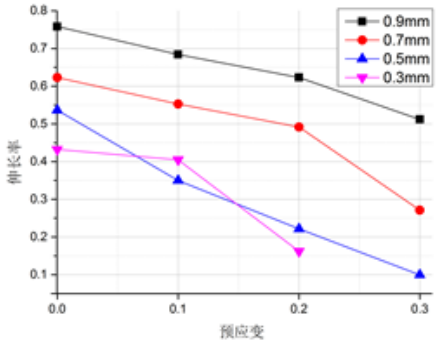

(a) Copper

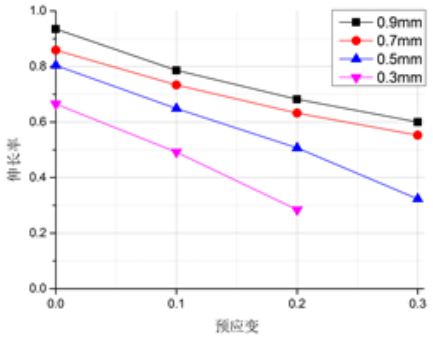

(b) Stainless Steel

Figure 17. The Elongation of Samples with Different Thickness and Pre-strain

Figure 17 shows the elongation at break for T2 copper and 0Cr18Ni9 stainless steel with different thicknesses under pre-strain. As shown, the thicker the sample is, the higher the elongation at break is; the pre-strain exerts great effects on the elongation at break of the material. The higher the pre-strain is, the higher the elongation at break for the material with same thicknesses is and the higher the plasticity is. Although the grain size is getting smaller when the pre-strain is increasing and the plasticity of the material can be enhanced, the cross-sectional area of the sample is reducing greatly by the pre-strain exerted and the plasticity of the sample is getting weak so it is easy to break.

4 CONCLUSION

A thin-walled semi-ellipsoidal shell unit was designed and the stamping forming process—deep drawing forming process is selected for preparing column cells with different materials and wall thickness. The finite element simulation is also used to study the effects of drawing forming on the thickness of the column cells. In addition, a deeper study is on the effects of pre-strain on the material performance caused by the forming process. The following conclusion are obtained.

(1) The finite element model established during the simulated pre-drawing process and it is in line with the actual processing. This is of great reference to the forming process for thin-walled semi-ellipsoidal shells.

(2) The deep drawing forming process can cause the reduction of the wall of the column cells, the longer the drawing distance is, the thinner the thickness is; the reduction of column cell wall for copper is more serious than the one for stainless steel and the wall thickness distribution is less constant; for the same sheet metal materials, the less the thickness is, the higher the flows stress is, under the same strain, and the lower the elongation at break is.

(3) The pre-strain distribution after the deep drawing forming process of the sheet metal is of significant inhomogeneity and larger plastic strain is produced at deeper parts. Under the same deep drawing condition, the maximum pre-strain of T2 copper column-cell was significantly higher than that of 0Cr18Ni9 stainless steel. And the pre-strain has significant effect on the plastic deformation

ability of the metal material. When the pre-strain increases, the yield strength of the material increases and the elongation at break decreases.

Acknowledgment

This work was supported by the National Natural Science Foundation of China (No. 11372355) and Military logistics research program (No. BY215J009) .

5 REFERENCES

►Altin, M., Güler, M. A., & Mert, S. K. (2017). The effect of percent foam fill ratio on the energy absorption capacity of axially compressed thin-walled multi-cell square and circular tubes. International Journal of Mechanical Sciences, s131–132: 368-379.

► Liu, Q.F., Cheng, X., Wang, N.C. (2015). A study on Mechanical Properties of Oxygen-free Copper under Impulsive Loadings. Mechanical Strength, 180(4): 607-612

►Cao, Y.J. (2014).Research on Deformation Prediction of Five-axis Machining Thin-walled Complex Surface. Dalian University of Technology.

►He, Z.D., Tian D.N. (2017). Control and Mechanical Analysis of Clamping Deformation of Thin-walled Spherical Shell Workpiece during Vacuum Suction, 38(7): 1409-1415.

►Jiang, X.H. (2014).Residual Stress Generation Mechanism and Control Method of Machining Accuracy of Complex Thin Wall Parts. Donghua University.

►Masmali, M., Mathew, P. (2017). An analytical approach for machining thin-walled workpieces ☆. Procedia Cirp, 58: 187-192.

►Panchagnula, J.S., Simhambhatla, S. (2018). Manufacture of complex thin-walled metallic objects using weld-deposition based additive manufacturing. Robotics and Computer-Integrated Manufacturing, 49: 194-203.

►Rezvani, M.J., Jafarian, B. (2017). An experimental investigation on energy absorption of thin-walled bitubal structures by inversion and axial collapse. International Journal of Mechanical Sciences, 126.

►Sun, G., Pang, T., Xu, C. (2017). Energy absorption mechanics for variable thickness thin-walled structures. Thin-Walled Structures, 118:214–228.

►Tang, Y.b. (2012). Research on Deformation Prediction Method of Thin-walled Structures Base on Finite Element Analysis. Harbin Institute of Technology: 20-28.

►Wang, X.S., Zhang, Y.H., Zhuang, H.Y. (2013).The Establishment and Simulation of Constitutive Equation on Advanced High Strength Steel. Automobile Technology & Material, 12: 1-5.

►Xiong, J., Li, R., Lei, Y., Chen, H. (2017). Heat propagation of circular thin-walled parts fabricated in additive manufacturing using gas metal arc welding. Journal of Materials Processing Technology, 251: 12-19

►Yin, Z.W., Zhang, X.H., Zhou, XJ, (2013).The Spinning Process of Large-scale Thin-walled Aluminum Alloy Hemisphere shell. Material Science and Technology, 21(4): 127-130.

►Zhao, X.J., Zhang, X.H., Yin, Z.W. (2012).The Formation Process of Long Diameter Thin-walled Aluminum Alloy shell. Hot working process, 41(19): 33-36.

►Zhu, X.Q., Liu, H. (2009). Dynamic Response of Simply Supported Sandwich Beams with Lattice Truss Cores Subjected to Impulsive Loadings. Acta Materiae Compositae Sinica, 26(1): 162-167.